

Ballistic thermal rectification in asymmetric three-terminal graphene nanojunctionsTao Ouyang,¹ Yuanping Chen,^{1,*} Yuee Xie,¹ X. L. Wei,¹ Kaike Yang,¹ Ping Yang,² and Jianxin Zhong^{1,†}¹Laboratory for Quantum Engineering and Micro-Nano Energy Technology, Xiangtan University, Xiangtan 411105, Hunan, China²Department of Physics and Optoelectronics, Taiyuan University of Technology, Taiyuan 030024, Shanxi, China

(Received 12 August 2010; revised manuscript received 22 October 2010; published 6 December 2010)

Graphene nanojunctions (GNJs) are important components of future nanodevices and nanocircuits. Using the nonequilibrium Green's function method, we investigate the phononic properties of three-terminal GNJs (TGNJs). The results show that the heat flux runs preferentially along the direction from narrow to wide terminals, presenting an evident ballistic thermal rectification effect in the asymmetric TGNJs. The rectification efficiency is strongly dependent on the asymmetry of the nanojunctions, which increases rapidly with the width discrepancy between the left and right terminals. Meanwhile, the corner form of the TGNJs also plays an important role in the rectification effect. The mechanism of this thermal rectification is explained by a qualitative analysis. Compared to previous thermal rectifiers based on other materials, the asymmetric nanojunctions based on graphene possess much high rectification ratio which can approach about 200%. These indicate that asymmetric TGNJs might be a promising candidate for excellent ballistic thermal (phononic) devices.

DOI: [10.1103/PhysRevB.82.245403](https://doi.org/10.1103/PhysRevB.82.245403)

PACS number(s): 81.05.ue, 65.80.Ck

I. INTRODUCTION

Phonons, long regarded as useless and harmful to electronic circuits, are found can be used to carry and process information recently.¹ Inspired by this progress, thermal (phononic) devices, e.g., thermal rectifiers,² thermal transistors,³ and thermal logical gates,⁴ have been proposed. Among these devices the thermal rectifier which can preferentially pass heat in one direction is the most fundamental component in phononic circuit.¹ Due to its great potential technological applications, numerous works have been performed to study the thermal rectification from various low-dimensional structures.²⁻¹³ Previous studies are mainly confined to the theoretical models based on nonlinear lattice.²⁻¹⁰ There is a little research investigating the thermal rectification in the actual materials. Merely recent few papers discussed the thermal rectification in carbon nanotube-based systems and the effect of rectification observed in these structures is not obvious.¹¹⁻¹³ Therefore it is desirable to find a nanomaterial with high rectification efficiency for fabricating promising thermal devices.

Graphene is a new type of single-atom layer carbon nanomaterial. Since prepared successfully in 2004, it has ignited tremendous interests because of the outstanding electronic properties.¹⁴⁻¹⁷ Recently superb thermal-transport properties have also been reported in graphene by both experimentally and theoretically.¹⁸⁻²⁰ Tailored or patterned from graphene sheet, various graphene nanostructures such as graphene nanoribbons (GNRs) and graphene nanojunctions (GNJs), can be easily fabricated.^{21,22} These graphene nanostructures present excellent thermal-transport properties as well and their thermal properties can be modulated by the structural size and geometry.²³⁻²⁸ The remarkable thermal properties lead us to envisage that graphene nanostructures may be potential candidates for designing thermal devices. Through molecular-dynamics simulations, Hu and Yang *et al.*^{27,28} demonstrate this conception from the asymmetric GNRs, in which excellent thermal rectification efficiency is shown. These breakthroughs arouse the great interest on the

thermal rectification effect of graphene and its derivatives. Recently, graphene is found to possess very long phonon mean-free path with experimental values about 775 nm at room temperature.^{18,19} This implies that the thermal transport in this unique carbon nanomaterial is nearly ballistic, especially when the temperature is not high and the geometric size is small. Therefore, the thermal transport in graphene nanostructures can be described by the Landauer formula.²³⁻²⁵ Under this scheme, for any two-terminal nanostructures the reverse of heat bath temperature will only result in the direction changes in heat fluxes while their magnitudes are equal to each other. That is, no ballistic thermal rectification effect can be achieved in the two-terminal graphene nanostructures. In order to obtain ballistic thermal rectification in graphene, one should turn attention to explore the phononic properties of the multiple-terminal graphene nanojunctions.

In this paper, we investigate the phononic properties in three-terminal graphene nanojunctions (TGNJs) as shown in Fig. 1. The heat fluxes in symmetric and asymmetric TGNJs are calculated first. It is found that the heat flux runs preferentially along the direction from narrow to wide terminals, presenting an evident thermal rectification effect in the asymmetric nanojunctions. By a qualitative analysis, the mechanism of this ballistic rectification in asymmetric TGNJs is explained. Then, the influence of geometric size on the rectification effect is discussed. The results show that the rectification efficiency is strongly dependent on the asymmetry of the TGNJs, which increases dramatically with the width difference between the left and right terminals. While the width of the control terminal plays a weak influence on the rectification ratio. In addition, we also study the thermal rectification in the TGNJs with flat corner and find that it is associated with the location and side height of corner. Compared to previous ballistic rectification models,²⁹ the graphene-based nanojunctions possesses more obvious rectification effect, and the rectification ratio can be as high as 200%. The results indicate that the asymmetric TGNJs can be used as important components for ballistic thermal devices.

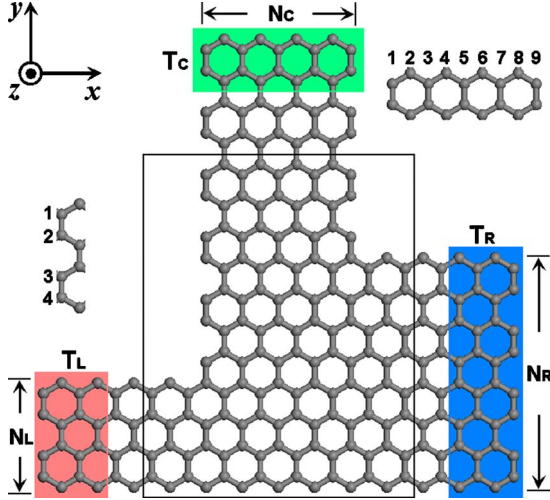


FIG. 1. (Color online) Schematic of an asymmetric TGNJ. The system is divided into four regions by the black frame: left, right, top semi-infinite thermal terminals, and a finite intersectional region. Among the three terminals, the left and right terminals are energy-input or energy-output leads while the top terminal is a control lead. The widths for the left, right, and control terminals are labeled by N_L , N_R , and N_C , respectively, and their temperatures are labeled by T_L , T_R , and T_C , respectively. The left (right) inset represents the definition of width for zigzag-edged (armchair-edged) terminal.

II. MODEL AND METHOD

Let us consider the TGNJ as shown in Fig. 1. The system can be divided into four regions by the black frame: three (left, right, and top) semi-infinite thermal terminals, and a finite intersectional region. Among the three thermal terminals, the left and right terminals are energy-input or energy-output leads, and the top terminal is a control lead. The widths for these terminals are labeled by N_L (left), N_R (right), and N_C (control), respectively. Following the conventional notation, the width of zigzag-edged (armchair-edged) terminal is determined by the number of zigzag carbon chains (carbon dimmer lines), as shown in the left (right) inset of Fig. 1. At a low temperature of several tens of kelvins, the thermal transport in graphene structure is dominantly carried by phonons,^{23–28,30} not by electrons, because recent experiment shows that all sub-ten-nanometer GNRs are semiconductor.³¹ In this unique carbon nanostructure, there exist three types of phonon modes: two in-plane (x - y plane) modes and one out-of-plane mode which is perpendicular to the x - y plane. Since out-of-plane mode in graphene shows no hybridization between the two in-plane modes, its Hamiltonian can be completely decomposed. Therefore, we mainly consider the thermal transport related to the out-of-plane mode in this paper. To describe the phonon properties of the TGNJs, one uses the harmonic approximation Hamiltonian

$$H = \sum_{\alpha=L,R,C,I} H_{\alpha} + \sum_{\beta=L,R,C} (u^{\beta})^T V^{\beta I} u^I, \quad (1)$$

where $H_{\alpha} = \frac{1}{2}(\dot{u}^{\alpha})^T \dot{u}^{\alpha} + \frac{1}{2}(u^{\alpha})^T K^{\alpha} u^{\alpha}$ represents coupled harmonic oscillators in region α . L , R , C , and I correspond to

the left, right, control terminals, and intersectional region, respectively. u^{α} is a column vector consisting of all the mass normalized displacement variables; \dot{u}^{α} is the corresponding conjugate momentum; K^{α} is the force constant matrix in the tight-binding form. The nearest-neighbor force constant is $k = 5.3 \text{ eV}/\text{\AA}^2$ while the next-nearest-neighbor interaction is estimated to be $k' = 0.265 \text{ eV}/\text{\AA}^2$.³⁰ The $V^{\beta I} = (V^{I\beta})^T$ in Eq. (1) is the coupling matrix of the terminal β to the intersectional region.

Based on this harmonic approximation Hamiltonian, the phonon transport properties of TGNJs can be calculated by using nonequilibrium Green's function (NEGF) method.³² According to the NEGF scheme, the retarded Green's function of this nanostructure can be expressed as

$$G^r = [(\omega + i0^+)^2 I - K^I - \Sigma_L^r - \Sigma_R^r - \Sigma_C^r]^{-1}, \quad (2)$$

where ω is the vibrational frequency of phonons and I is an identity matrix. The $\Sigma_{\beta}^r = V^{I\beta} g_{\beta}^r V^{\beta I}$ denotes the self-energy of terminal β and g_{β}^r is the terminal surface Green's function. Here the g_{β}^r is calculated by: $g_{\beta}^r = [(\omega + i0^+)^2 I - K_{00}^{\beta} - K_{01}^{\beta} \Lambda]^{-1}$ (Refs. 32 and 33) with K_{00}^{β} and K_{01}^{β} are the force constant and coupling matrices for a unit cell in terminal β . The Λ is the appropriate transfer matrix, which can be calculated from the force constant matrix element via an iterative procedure.³³ Once the retarded Green's function G^r is obtained, we can calculate phonon transmission $\tau_{\beta\alpha}$ (from terminal α to terminal β , here $\tau_{\beta\alpha} = \tau_{\alpha\beta}$ because of time-reversal symmetry), thermal conductance $\sigma_{\beta\alpha}$ and heat flux $J_{\beta\alpha}$ (Ref. 32)

$$\tau_{\beta\alpha}[\omega] = \text{Tr}\{G^r \Gamma_{\alpha} G^{\alpha} \Gamma_{\beta}\}, \quad (3a)$$

$$\sigma_{\beta\alpha} = \frac{1}{2\pi} \int_0^{\infty} \tau_{\beta\alpha} \cdot \omega \cdot \frac{\partial f(\omega)}{\partial T} \cdot d\omega, \quad (3b)$$

$$J_{\beta\alpha} = \frac{\hbar}{2\pi} \int_0^{\infty} \tau_{\beta\alpha} \cdot \omega \cdot [f(T_{\alpha}) - f(T_{\beta})] \cdot d\omega, \quad (3c)$$

where $\Gamma_{\beta} = i(\Sigma_{\beta}^r - \Sigma_{\beta}^a) = -2 \text{Im} V^{I\beta} g_{\beta}^r V^{\beta I}$ is the coupling function of the β terminal, and $f(T_{\beta}) = \{\exp[\hbar\omega/(k_B T_{\beta})] - 1\}^{-1}$ is Bose-Einstein distribution function for heat carriers at the terminal.

In our calculation, the left and right terminals are coupled to the thermal reservoir and their temperatures are T_L and T_R , respectively. While the control terminal is coupled to a temperature probe hold fixed temperature T_C . It means that the control terminal is reached the steady state³⁴ and there is no heat flux flowing through this lead

$$J_C = J_{CL}(T_L, T_C) + J_{CR}(T_R, T_C) = 0. \quad (4)$$

Such a control terminals, which is referred to as Buttiker's probe,^{35,36} gives a weak effect of phonon-phonon scattering on the heat flux flowing between the left and right terminals. Although this effect is limited,²⁹ the phonon transmission from left to right terminals $\tau_{RL}(\omega)$ is still amended in our simulation for describing the thermal transport in the three-terminal nanojunctions more reasonable. According to the Ref. 35, the modified transmission $\tau_{RL}^M(\omega)$ including the phonon-phonon scattering is given by: $\tau_{RL}^E(\omega) = \tau_{RL}(\omega)$

$+\tau_{CL}(\omega) \cdot \tau_{RC}(\omega) / [\tau_{CL}(\omega) + \tau_{RC}(\omega)]$. Here the temperature of control terminal is limited lower than the Debye temperature of graphene³⁷ to ensure that the phonon transport in the structure is ballistic. For a given control temperature T_C , pairs of corresponding temperatures T_L and T_R can be obtained from Eq. (4), which are used to calculate the heat flux between any two terminals in the system. During studies the thermal rectification, the heat fluxes of two cases are considered. In the first case $T_L > T_R$, the heat fluxes flow from left to right terminals J_{RL} and from control to right terminals J_{RC} , the total heat flux flows into the right terminal is denoted as J_+ ($J_+ = J_{RL} + J_{RC}$). In the inverse case with $T_L < T_R$, the heat fluxes flow from right to left terminals J_{LR} and from control to left terminals J_{LC} , the total heat flux flows into the left terminal is denoted as J_- ($J_- = J_{LR} + J_{LC}$). As stated above, one can get all values of the heat flux J_+ and J_- corresponding to different temperature pairs of T_L and T_R . When the absolute value of temperature bias ΔT [$\Delta T = (T_L - T_R) / 2T_C$] between the left and right terminals is equal, the rectification ratio R can be calculated²⁹

$$R = \text{abs}(J_+ - J_-) / \min(J_+, J_-). \quad (5)$$

III. RESULTS AND DISCUSSION

In Fig. 2(a) the heat fluxes J_+ and J_- as a function of temperature bias ΔT for the asymmetric TGNJ are described by the square symbol while the heat fluxes for the symmetric TGNJ are described by the circle symbol for convenience of comparison. One can find that the heat fluxes J_+ and J_- for the symmetric TGNJ are symmetric with the axis of $\Delta T = 0$ owing to the intrinsic structure characteristic. With temperature bias ΔT ascending, since more optical phonons are frozen out and contribute to the thermal transport, both the heat fluxes J_+ and J_- increase simultaneously. At the same absolute value of temperature bias $|\Delta T|$, the heat fluxes J_- and J_+ only change direction while their values are equal to each other. That is, the heat flux of the symmetric TGNJ flows from left to right terminals is the same as that flows from right to left terminals. However, the heat fluxes for the asymmetric TGNJ display distinct behavior [see the square symbol in Fig. 2(a)]. The fluxes J_+ and J_- are asymmetric with the axis of $\Delta T = 0$. As the temperature of left terminal T_L is higher ($\Delta T > 0$), the heat flux J_+ increases steeply with temperature bias. While in the case $\Delta T < 0$, the heat flux J_- varies slowly with temperature bias by comparing to the J_- of symmetric junction. At the same $|\Delta T|$, it can be seen clearly that the heat flux J_+ is larger than the J_- . This implies that the heat flux prefers to flow from left to right terminals in this asymmetric system, presenting an obvious ballistic thermal rectification effect. Figure 2(b) shows the thermal rectification ratio R for the two types of TGNJs. For the symmetric structure, the rectification ratio is zero due to the symmetric heat fluxes J_+ and J_- . Nevertheless, for the asymmetric case the rectification efficiency increases rapidly with the temperature bias. As $|\Delta T|$ approaches 0.5, the rectification ratio is about 45% which is larger than the biggest rectification efficiency in previous ballistic thermal rectification models ($\sim 5\%$).²⁹ These results indicate that one can achieve

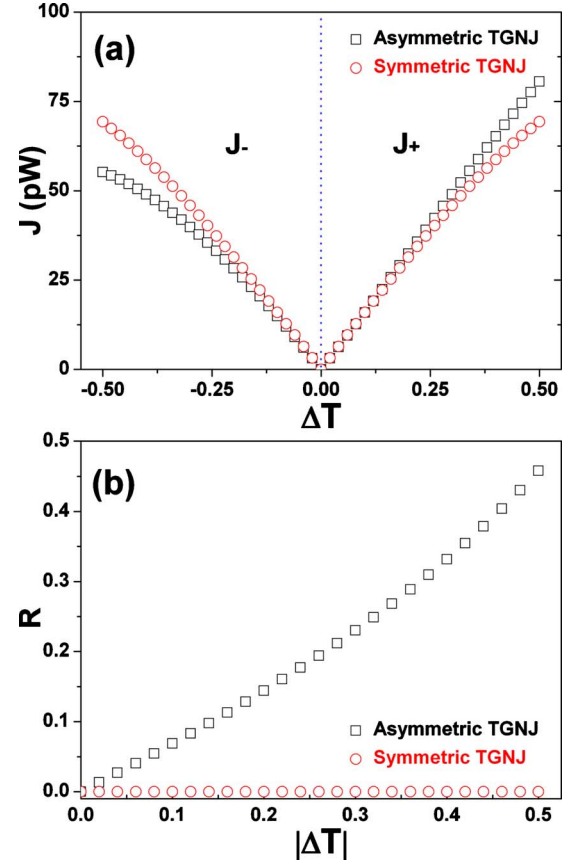


FIG. 2. (Color online) (a) The heat flux J_+ ($\Delta T > 0$) and J_- ($\Delta T < 0$) as a function of temperature bias ΔT for an asymmetric TGNJ ($N_L = 4$, $N_R = 8$) and a symmetric TGNJ ($N_L = 4$, $N_R = 4$). (b) The rectification ratio R versus $|\Delta T|$ corresponding to the asymmetric and symmetric TGNJ in Fig. 2(a). Other parameters are chosen as: $N_C = 9$ and $T_C = 10$ K.

evident ballistic thermal rectification in the asymmetric TGNJ.

To elucidate the origination of the ballistic rectification effect in the asymmetric TGNJ, a qualitative analysis is given as below. The thermal rectification ratio R of a nanosystem mainly depends on the difference between the heat fluxes J_+ and J_- , according to the Eq. (5). It means that the rectification efficiency relies on the discrepancy of thermal transport properties of two cases, i.e., $\Delta T > 0$ and $\Delta T < 0$. For convenience of description in the following, the superscripts + and - are employed to distinguish the physical parameters of the cases with $\Delta T > 0$ (+) and $\Delta T < 0$ (-). For example, T_L^+ , T_R^+ and $\Delta T^+ = (T_L^+ - T_R^+) / 2T_C$ represent the temperatures of left, right terminals and temperature bias as $\Delta T > 0$, respectively. While T_L^- , T_R^- , and ΔT^- represent the temperature of left, right terminals, and temperature bias as $\Delta T < 0$, respectively. In both cases, the control terminal should satisfy the condition of steady state in Eq. (4) all along. Because the temperature difference between any two terminals is small in our calculation, the heat-flux equation [Eq. (3c)] can be expressed as $J_{\beta\alpha} = \sigma_{\beta\alpha}(T_\alpha - T_\beta)$.³⁸ Correspondingly, the Eq. (4) is rewritten as

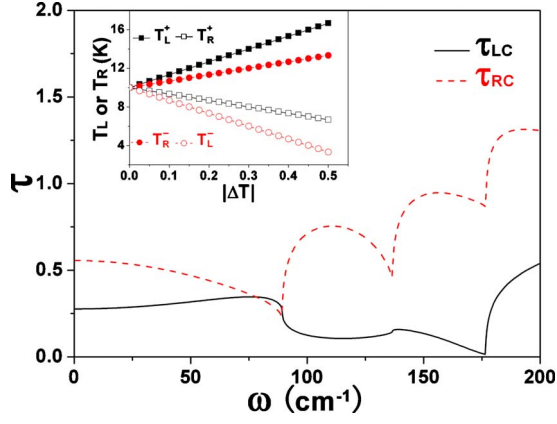


FIG. 3. (Color online) The phonon transmission τ_{CR} (from right to control terminals) and τ_{CL} (from left to control terminals) as a function of vibrational frequency ω for an asymmetric TGNJ with $N_L=4$, $N_R=8$, and $N_C=9$. Inset of (a): the temperatures $T_L^{+/-}$ and $T_R^{+/-}$ as a function of $|\Delta T|$, the parameters are chose as: $\gamma=2$, $T_C=10$ K. The superscripts + and - respectively represent the two cases with $\Delta T>0$ and $\Delta T<0$.

$$J_C = \sigma_{CL}(T_L - T_C) + \sigma_{CR}(T_R - T_C) = 0. \quad (6)$$

Thus, based on the Eq. (6), the relationship among the temperatures of left and right terminals, and the temperature bias in the first case $\Delta T>0$ can be obtained

$$\Delta T^+ = (\gamma + 1)(T_L^+ - T_C)/2\gamma T_C, \quad (7a)$$

$$T_R^+ = [(\gamma + 1)T_C - T_L^+]/\gamma \quad (7b)$$

with $\gamma = \sigma_{CR}^+/\sigma_{CL}^+$. Similarly, in the other case $\Delta T<0$, one can get

$$\Delta T^- = (\gamma' + 1)(T_C - T_R^-)/2T_C, \quad (8a)$$

$$T_L^- = (\gamma' + 1)T_C - \gamma' T_R^- \quad (8b)$$

with $\gamma' = \sigma_{CR}^-/\sigma_{CL}^-$ ($\gamma' \approx \gamma$ due to the small temperature and temperature bias). Then using the condition $|\Delta T^+| = |\Delta T^-|$, the relationship between T_L^+ and T_R^- is built by solving Eqs. (7a) and (8a)

$$\begin{aligned} (\gamma + 1)(T_L^+ - T_C)/\gamma T_C &= (\gamma + 1)(T_R^- - T_C)/T_C \Rightarrow T_L^+ - T_C \\ &= \gamma(T_R^- - T_C). \end{aligned} \quad (9)$$

From Eq. (9) one can found that the magnitude between T_L^+ and T_R^- is determined by the value of $\gamma = \sigma_{CR}/\sigma_{CL}$. While the thermal conductance is closely related to phonon transmission coefficient, i.e., the transmission from right to control terminals τ_{CR} and left to control terminal τ_{CL} need to be determined first before estimating the value of γ . In Fig. 3, the transmission τ_{CR} and τ_{CL} for an asymmetric TGNJ is given. It is shown that the transmission τ_{CL} is quite lower than the τ_{CR} since the left terminal is narrower than the right one. In turn, the thermal conductance from left to right terminal σ_{CL} is smaller than that from right to control terminal σ_{CR} with the resultant $\gamma>1$. Finally, substituting the value of γ into the Eq. (9), the temperature relationship between the two cases can be derived: $T_L^+>T_R^-$; and $T_R^+>T_L^-$ can

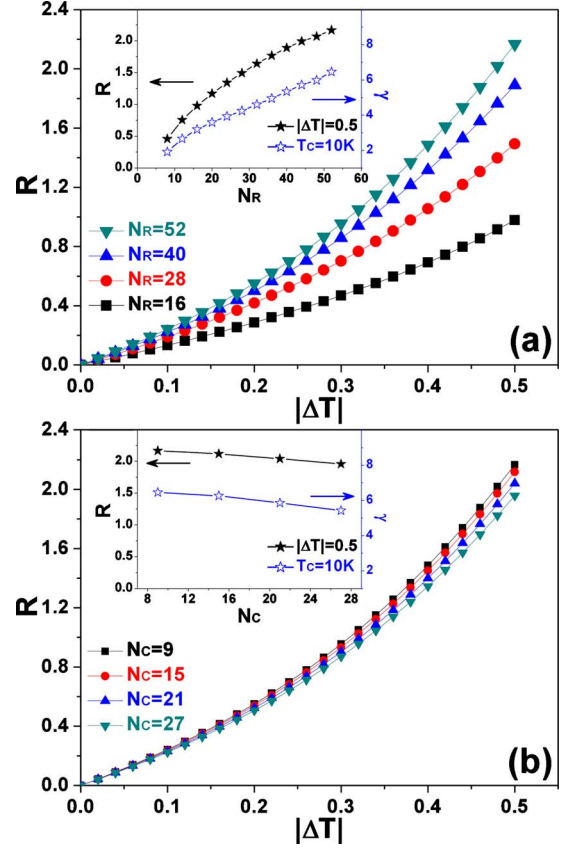


FIG. 4. (Color online) The rectification ratio R as a function of temperature bias $|\Delta T|$ for asymmetric TGNJs with (a) different widths of right thermal terminal N_R ($N_L=4$, $N_C=9$, and $T_C=10$ K); (b) different widths of control terminal N_C ($N_L=4$, $N_R=52$, and $T_C=10$ K). Inset of (a): the rectification ratio R and thermal conductance ratio γ ($\gamma = \sigma_{CR}/\sigma_{CL}$) versus the width of right thermal terminal N_R . Inset of (b): the R and γ versus the width of control terminal N_C .

be obtained as well in a similar way. Namely, the T_L^+ (T_R^+) is always bigger than T_R^- (T_L^-) at the same temperature bias, which can be seen clearly in the inset of Fig. 3. It suggests that in the case of $\Delta T>0$, more phonon modes with higher energy can be excited and contribute to the thermal transport. As a result, the thermal conductance from left to right terminal σ_{LR}^+ is larger than the σ_{LR}^- . This demonstrates that the heat flux runs preferentially along the direction of left to right terminals and thus obvious ballistic thermal rectification effect is generated in the asymmetric TGNJs.

In Fig. 4 we plot the effect of geometric size on the thermal rectification ratio of asymmetric TGNJs. The thermal rectification ratio R for the asymmetric TGNJs as a function of temperature bias ΔT with different widths of right terminal N_R is depicted in Fig. 4(a). One can find that all the rectification ratio increase with the temperature bias ΔT , just like the discussion presented in Fig. 2(b). Meanwhile, the increase of width for right terminal N_R results in the dramatically increase in thermal rectification efficiency. To show this behavior more directly, the rectification ratio R versus the width of right terminal N_R is depicted by the solid symbol in the inset of Fig. 4(a). The rectification ratio of the asymmet-

ric nanojunctions increases from 45% to 216% as the widths of right terminal increase from $N_R=8$ to $N_R=52$. It can be expected that the rectification efficiency will be further improved by increasing the widths of right terminal. This behavior can be explained as follows. For a fixed left thermal terminal, the increasing widths of right terminal will enhance the asymmetry of the nanojunction. According to the analysis mentioned above, the enhanced asymmetry will induce more evident discrepancy of phonon transmission between τ_{CR} and τ_{CL} , and thus leading to more distinct thermal conductance ratio γ ($\gamma=\sigma_{CR}/\sigma_{CL}$) in the asymmetric TGNJs [see the hollow symbol in the inset of Fig. 4(a)]. Consequently, the rectification ratio increases with the width difference between left and right terminals.

Figure 4(b) shows the effect of width for control terminal N_C on the thermal rectification efficiency. It can be found that the geometric size of control terminal plays a weak influence on the rectification ratio R . This phenomenon is illustrated more clearly by the solid symbol in the inset of Fig. 4(b). The rectification ratio R still can approach 195% even in the asymmetric TGNJs with wide control terminal. It is originated from the fact that although the thermal conductance σ_{CR} and σ_{CL} will varies with the width of control terminal, the ratio between them γ ($\gamma=\sigma_{CR}/\sigma_{CL}$) will not emerge evident changes [see the hollow symbol in the inset of Fig. 4(b)]. As a result, the thermal rectification efficiency is nearly independent on the width of control terminal. From the results presented in Fig. 4(b), one can conclude that the control terminal just acts as a temperature probe in the rectification process, which will not break the thermal rectification effect in the asymmetric TGNJs.

In addition, the effect of corner form on the thermal rectification of asymmetric TGNJ is also explored. Compared to the former TGNJs with sharp corners, herein we mainly consider two types of deformed TGNJs with flat corners. One is the TGNJ with armchair-edged corner between the left and control terminals, which is called type L with side height N_H^L (shown in the left inset of Fig. 5). The other is the TGNJ with armchair-edged corner between the right and control terminals, which is called type R with side height N_H^R (shown in the right inset of Fig. 5). The rectification ratio R versus the side height of corner $N_H^{L/R}$ for the two types of asymmetric TGNJs is plotted by the solid symbols in Fig. 5. One can see that the ballistic thermal rectification efficiency displays quite different side height dependent for the two types of nanojunctions. As to the type L , the thermal rectification efficiency decreases rapidly with increasing the side height of corner N_H^L . It is attributed to the fact that increasing the N_H^L will remarkable reduces the asymmetry between the left and right terminals, and then leads to the decreasing of thermal conductance ratio γ between the two terminals. Hence the rectification ratio decreases as the side height N_H^L increases. On the contrary, the thermal rectification efficiency for the type R increases with the side height of corner N_H^R due to the enhancement of asymmetry for the TGNJs. Similarly phenomenon can be further confirmed by investigating the thermal rectification of the asymmetric TGNJs with zigzag corner (the data are not shown). These results suggest that one can further modulate the thermal rectification by varying the geometric size of the corner form.

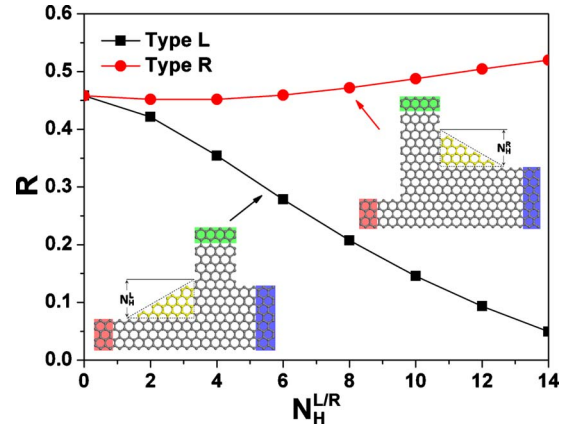


FIG. 5. (Color online) The rectification ratio R versus the side height of corner $N_H^{L/R}$ for the two types of asymmetric TGNJs with armchair-edged corner (the dashed triangle-frame denotes the corner part). The geometry for the two types of TGNJs: type L and type R , are, respectively, sketched in the left and right inset of Fig. 5. The $N_H^{L/R}$ denotes the number of zigzag carbon chains, which represents the side height of corner for the type L or type R . Other parameters are chose as: $N_L=4$, $N_R=8$, $N_C=9$, and $T_C=10$ K.

IV. CONCLUSIONS

In summary, using nonequilibrium Green's function method, the phononic properties of TGNJs are investigated. We first calculate the heat fluxes in symmetric and asymmetric TGNJs. It is shown that the heat flux runs preferentially along the direction from narrow to wide terminals, presenting an evident ballistic thermal rectification effect in the asymmetric TGNJs. The rectification efficiency is strongly dependent on the asymmetry of the nanojunction, which increases rapidly with the width discrepancy between the left and right terminals. Nevertheless the geometric size of control terminal plays a weak influence on the rectification ratio. In addition, we also discuss the thermal rectification of the TGNJs with armchair-edged corner and find that it is associated with the location and side height of corner, which provides another way to modulate the rectification efficiency. By a qualitative analysis, the mechanism for the ballistic rectification in asymmetric TGNJs is obtained explanation. Compared to previous thermal rectifiers based on other materials, the asymmetric nanojunctions based on graphene can induce more obvious rectification effect and the rectification ratio can be as high as 200%. The results could offer useful guidelines to the design and performance improvement of the graphene-based ballistic thermal rectifier.

ACKNOWLEDGMENTS

This work was supported by the Cultivation Fund of the Key Scientific and Technical Innovation Project, Ministry of Education of China (Grant No. 708068), the Open Fund based on innovation platform of Hunan colleges and universities (Grant No. 09K034), the National Natural Science Foundation of China (Grant Nos. 51006086 and 11074213), and the Hunan Provincial Innovation Foundation for Postgraduate (Grant No. CX2010B253).

*chenyp@xtu.edu.cn

†jxzhong@xtu.edu.cn

- ¹L. Wang and B. Li, *Phys. World* **21** (3), 27 (2008).
- ²B. Li, L. Wang, and G. Casati, *Phys. Rev. Lett.* **93**, 184301 (2004); D. Segal and A. Nitzan, *ibid.* **94**, 034301 (2005); G. Casati, *Chaos* **15**, 015120 (2005); M. Terraneo, M. Peyrard, and G. Casati, *Phys. Rev. Lett.* **88**, 094302 (2002).
- ³B. Li, L. Wang, and G. Casati, *Appl. Phys. Lett.* **88**, 143501 (2006).
- ⁴L. Wang and B. Li, *Phys. Rev. Lett.* **99**, 177208 (2007).
- ⁵J. P. Eckmann and C. Mejia-Monasterio, *Phys. Rev. Lett.* **97**, 094301 (2006).
- ⁶B. Hu, L. Yang, and Y. Zhang, *Phys. Rev. Lett.* **97**, 124302 (2006).
- ⁷G. Casati, C. Mejia-Monasterio, and T. Prosen, *Phys. Rev. Lett.* **98**, 104302 (2007).
- ⁸D. Segal, *Phys. Rev. Lett.* **100**, 105901 (2008).
- ⁹L. Wang and B. Li, *Phys. Rev. Lett.* **101**, 267203 (2008).
- ¹⁰L. A. Wu and D. Segal, *Phys. Rev. Lett.* **102**, 095503 (2009).
- ¹¹C. W. Chang, D. Okawa, A. Majumdar, and A. Zettl, *Science* **314**, 1121 (2006).
- ¹²G. Wu and B. Li, *Phys. Rev. B* **76**, 085424 (2007).
- ¹³N. Yang, G. Zhang, and B. Li, *Appl. Phys. Lett.* **93**, 243111 (2008).
- ¹⁴Y. Zhang, Y. W. Tan, H. L. Stormer, and P. Kim, *Nature (London)* **438**, 201 (2005).
- ¹⁵K. S. Novoselov, Z. Jiang, Y. Zhang, S. V. Morozov, H. L. Stormer, U. Zeitler, J. C. Maan, G. S. Boebinger, P. Kim, and A. K. Geim, *Science* **315**, 1379 (2007).
- ¹⁶A. H. Castro Neto, F. Guinea, N. M. R. Peres, K. S. Novoselov, and A. K. Geim, *Rev. Mod. Phys.* **81**, 109 (2009).
- ¹⁷Y. P. Chen, Y. E. Xie, L. Z. Sun, and J. X. Zhong, *Appl. Phys. Lett.* **93**, 092104 (2008); Y. P. Chen, Y. E. Xie, and X. H. Yan, *J. Appl. Phys.* **103**, 063711 (2008).
- ¹⁸S. Ghosh, I. Calizo, D. Teweldebrhan, E. P. Pokatilov, D. L. Nika, A. A. Balandin, W. Bao, F. Miao, and C. N. Lau, *Appl. Phys. Lett.* **92**, 151911 (2008).
- ¹⁹A. A. Balandin, S. Ghosh, W. Bao, I. Calizo, D. Teweldebrhan, F. Miao, and C. N. Lau, *Nano Lett.* **8**, 902 (2008).
- ²⁰S. Ghosh, W. Bao, D. L. Nika, S. Subrina, E. P. Pokatilov, C. N. Lau, and A. A. Balandin, *Nature Mater.* **9**, 555 (2010).
- ²¹K. S. Novoselov, A. K. Geim, S. V. Morozov, D. Jiang, Y. Zhang, S. V. Dubonos, I. V. Grigorieva, and A. A. Firsov, *Science* **306**, 666 (2004).
- ²²C. Berger, Z. M. Song, X. B. Li, X. S. Wu, N. Brown, C. Naud, D. Mayou, T. B. Li, J. Hass, A. N. Marchenkov, E. H. Conrad, P. N. First, and W. A. de Heer, *Science* **312**, 1191 (2006).
- ²³J. H. Lan, J. S. Wang, C. K. Gan, and S. K. Chin, *Phys. Rev. B* **79**, 115401 (2009); J. W. Jiang, J. S. Wang, and B. Li, *ibid.* **79**, 205418 (2009).
- ²⁴T. Ouyang, Y. P. Chen, K. K. Yang, and J. X. Zhong, *EPL* **88**, 28002 (2009); K. K. Yang, Y. P. Chen, Y. E. Xie, T. Ouyang, and J. X. Zhong, *ibid.* **91**, 46006 (2010).
- ²⁵Y. Xu, X. B. Chen, J. S. Wang, B. L. Gu, and W. H. Duan, *Phys. Rev. B* **81**, 195425 (2010); Y. Xu, X. Chen, B.-L. Gu, and W. Duan, *Appl. Phys. Lett.* **95**, 233116 (2009).
- ²⁶J. N. Hu, S. Schiffl, A. Vallabhaneni, X. L. Ruan, and Y. P. Chen, *Appl. Phys. Lett.* **97**, 133107 (2010); Z. Tan, J. Wang, and C. Gan, *arXiv:1007.1831* (unpublished).
- ²⁷J. N. Hu, X. L. Ruan, and Y. P. Chen, *Nano Lett.* **9**, 2730 (2009).
- ²⁸N. Yang, G. Zhang, and B. W. Li, *Appl. Phys. Lett.* **95**, 033107 (2009).
- ²⁹L. Zhang, J.-S. Wang, and B. Li, *Phys. Rev. B* **81**, 100301 (2010); Y. Ming, Z. Wang, Z. Ding, and H. Li, *New J. Phys.* **12**, 103041 (2010).
- ³⁰M. Morooka, T. Yamamoto, and K. Watanabe, *Phys. Rev. B* **77**, 033412 (2008); T. Yamamoto, K. Watanabe, and K. Mii, *ibid.* **70**, 245402 (2004).
- ³¹X. Li, X. Wang, L. Zhang, S. Lee, and H. Dai, *Science* **319**, 1229 (2008).
- ³²N. Mingo, *Phys. Rev. B* **74**, 125402 (2006); T. Yamamoto and K. Watanabe, *Phys. Rev. Lett.* **96**, 255503 (2006); J. S. Wang, J. Wang, and J. T. Lü, *Eur. Phys. J. B* **62**, 381 (2008).
- ³³M. P. L. Sancho, J. M. L. Sancho, and J. Rubio, *J. Phys. F: Met. Phys.* **15**, 851 (1985).
- ³⁴P. Yang, W. R. Zhong, Y. F. He, and B. Hu, *J. Appl. Phys.* **107**, 094309 (2010); P. Yang and B. Hu, *arXiv:0908.0422* (unpublished).
- ³⁵T. Yamamoto, S. Konabe, J. Shiomi, and S. Maruyama, *Appl. Phys. Express* **2**, 095003 (2009).
- ³⁶M. Büttiker, *Phys. Rev. B* **33**, 3020 (1986).
- ³⁷F. Liu, P. Ming, and J. Li, *Phys. Rev. B* **76**, 064120 (2007); V. K. Tewary and B. Yang, *ibid.* **79**, 125416 (2009).
- ³⁸Q. F. Sun, P. Yang, and H. Guo, *Phys. Rev. Lett.* **89**, 175901 (2002).